Supporting Information for:

Capturing the Long-Sought Small-Bandgap Endohedral Fullerene $Sc_3N@C_{82}$ with Low Kinetic Stability

Tao Wei,[a] Song Wang,[a] Fupin Liu,[a] Yuanzhi Tan,[b] Xianjun Zhu,[a] Suyuan Xie,[b] and Shangfeng Yang*[a]

[a] Hefei National Laboratory for Physical Sciences at Microscale, CAS Key Laboratory of Materials for Energy Conversion, Department of Materials Science and Engineering, Synergetic Innovation Center of Quantum Information & Quantum Physics, University of Science and Technology of China (USTC), Hefei 230026, China

[b] State Key Laboratory of Physical Chemistry of Solid Surfaces and Department of Chemistry, College of Chemistry and Chemical Engineering, Xiamen University, Xiamen 361005, China

Content

S1. Isolation of $Sc_3N@C_{82}$.

$Sc_3N@C_{82}$ was synthesized in a modified Krätschmer-Huffman generator by vaporizing composite graphite rods (Φ8 × 150 mm) containing a mixture of Sc_2O_3 (99.99%) and graphite powder with a molar ratio of 1:15 (Sc:C) with the addition of 10 mbar N_2 into 400 mbar He. The as-produced soot was Soxhlet-extracted by CS_2 for 24 h, and the resulting brown-yellow solution was distilled to remove CS_2 and then immediately redissolved in toluene (~200 ml) and subsequently passed through a 0.2 μm Telflon filter (Sartorius AG, Germany) for HPLC isolation. $Sc_3N@C_{82}$ was isolated by three-step HPLC as illustrated in Fig. S1. In the first step, the fullerene extract mixture was isolated by 20 × 250 mm Buckyprep column, and fraction **A** with retention time ranging from 47.5 to 52.3 min was collected (see Fig. S1(a)). In the second-step isolation, the collected fraction **A** was subjected to the recycling HPLC isolation running in a 10 × 250 mm Buckyprep-M column, and fraction **A-1** was collected after two cycles (see Fig. S1(b)). In the third step, fraction **A-1** was further isolated by recycling HPLC using 10 × 250 mm Buckyprep column, resulting in isolation of fraction **A-1-1**, which was further checked by LD-TOF MS measurement as shown in Figure S2.

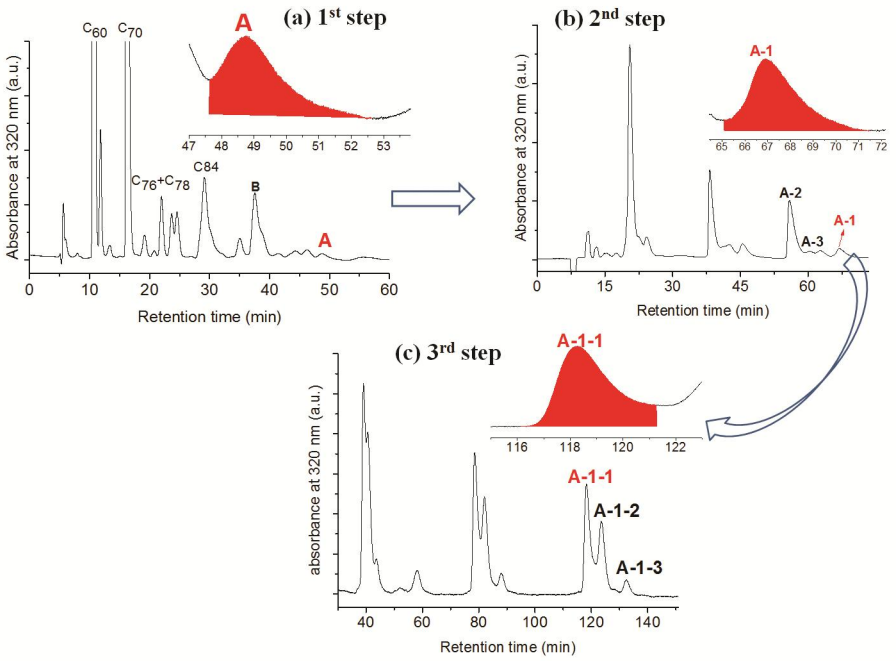

Figure S1. Isolation scheme of $Sc_3N@C_{82}$. (a) Chromatogram of the fullerene extract mixture obtained from Sc_2O_3 with addition of N_2. (20 × 250 mm Buckyprep column; flow rate: 15 mL·min^{-1}; injection volume: 15 mL; toluene as eluent; 40 °C.) (b) Recycling HPLC chromatogram of fractions **A** isolated from the Sc_2O_3/N_2 extract (10 × 250 mm Buckyprep-M column; flow rate 5.0 ml/min; injection volume 5 ml; toluene as eluent; 40 °C). (c) Recycling HPLC chromatogram of fraction **A-1** (10 × 250 mm Buckyprep column; flow rate 5.0 ml/min; injection volume 5 ml; toluene as eluent; 40 °C). Inset: Enlarged chromatogram regions highlighting the fractions to be collected for next-step isolation. **A-1-1**: $Sc_3N@C_{82}$; **A-1-2**: $Sc_3CN@C_{80}$; **A-1-3**: Sc_3CNC_{82}; **A-2**: C_{92}; **A-3**: $Sc_2@C_{86}$; **B**: $Sc_3N@C_{80}$ (I)+ $Sc_3N@C_{80}$ (II)+C_{86}.

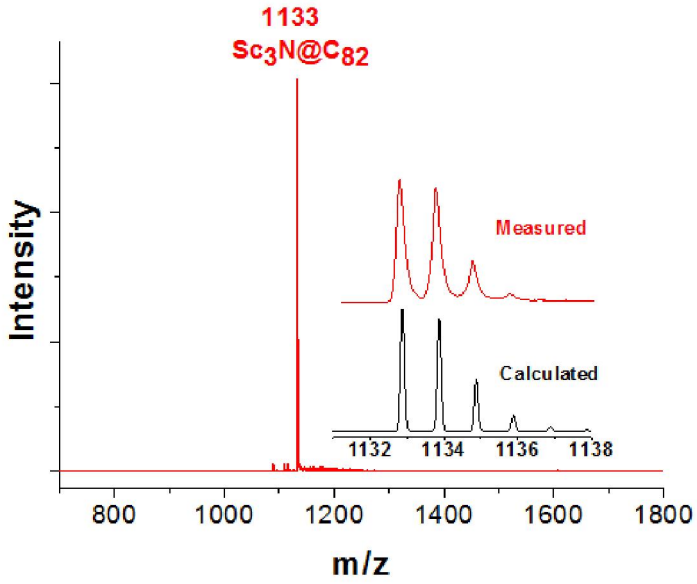

Figure S2. Postive-ion laser desorption time-of-flight (LD-TOF) mass spectrum of the isolated $Sc_3N@C_{82}$ (Fraction **A-1-1**). Insets: measured and calculated isotopic distributions of $Sc_3N@C_{82}$.

S2. Estimation of the relative yield of $Sc_3N@C_{82}$ to $Sc_3N@C_{80}$ (I_h) and $Sc_3N@C_{70}$.

The relative yield of $Sc_3N@C_{82}$ to $Sc_3N@C_{80}$-I_h and $Sc_3N@C_{70}$ is estimated based on the integration area of the corresponding peaks in the chromatograms shown in Fig. S1.

Table S1. Assignments of each (sub)fraction and their relative abundance.

Fraction	Sub-fraction	Major component	Relative abundance
B	-	$Sc_3N@C_{80}$-I_h	79.1%
		$Sc_3N@C_{80}$-D_{5h}	13.2%
		C_{86}	7.7%
A	**A-1**	$Sc_3N@C_{82}$, $Sc_3CN@C_{80}$	8.4%
	A-2 + **A-3**	C_{92} + Sc_2C_{86}	91.6%
A-1	**A-1-1**	**$Sc_3N@C_{82}$**	48.6%
	A-1-2 + **A-1-3**	$Sc_3CN@C_{80}$, Sc_3CNC_{82}	51.4%

(1) Given that relative yield of fraction **A**:**B** is 12.1%:1, the relative yield of $Sc_3N@C_{82}$ to $Sc_3N@C_{80}$-I_h can be calculated as:

$Sc_3N@C_{82}/Sc_3N@C_{80}$-$I_h$ = 48.6% × 8.4% × 12.1% / 79.1% ≈ 0.62%

(2) In our previous work, the relative yield of $Sc_3N@C_{68}$ to $Sc_3N@C_{80}$-I_h and $Sc_3N@C_{70}$ to $Sc_3N@C_{68}$ was calculated to be 1:10 and 1.8%:1, respectively.[S1] Thus, the relative yield of $Sc_3N@C_{82}$ relative to $Sc_3N@C_{70}$ can be calculated as:

$Sc_3N@C_{70}/Sc_3N@C_{80}$-$I_h$ = 1.8% ÷ 10 = 0.18%

$Sc_3N@C_{82}/Sc_3N@C_{70}$ = 0.62% / 0.18% ≈ 3.4:1

S3. X-ray crystallographic data of $Sc_3N@C_{82}$-C_{2v}(39718).

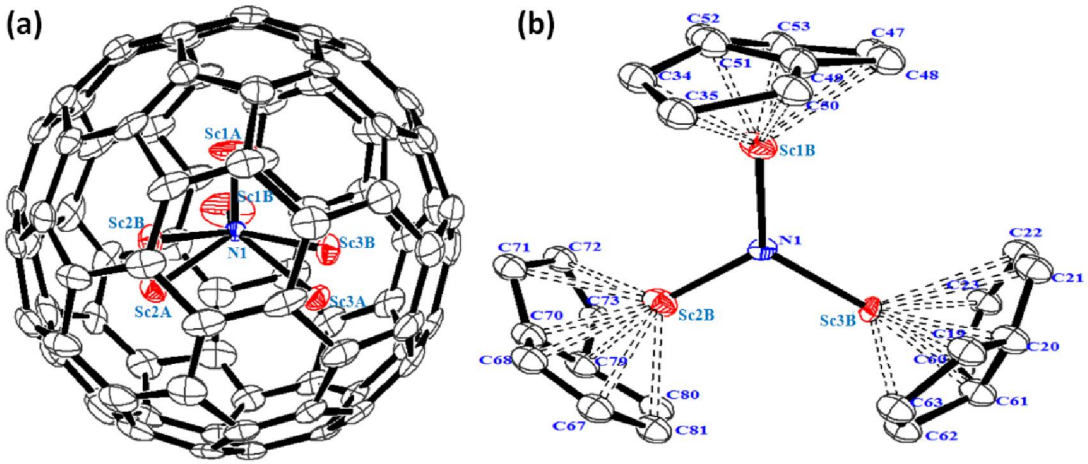

Figure S3. (a) Drawing showing the relative position of two Sc_3N sites inside the C_{82}-C_{2v}(39718) cage, including the major one composed of Sc1A-Sc3A and the minor one consisting of Sc1B-Sc3B. All atoms are shown in 30% thermal ellipsoids. (b) Position of the minor Sc_3N site with respect to the nearest carbon atoms of C_{2v}(39718)-C_{82} cage. C, N and Sc atoms are shown in gray, blue and red, respectively.

Table S2. Crystal and structure data of $Sc_3N@C_{82}$-C_{2v}(39718) at 100 K.

Temperature	T = 100 K	Crystal size	0.1 × 0.08 × 0.06 mm^3
Empirical formula	C131 H56 N5 Ni Sc3	Reflections collected	7517
Formula weight	1890.40	Independent reflections	6807[R(int) = 0.0374]
Wavelength	1.54178	Completeness to θ	98.7% (θ = 70.79)
Space group	C 2/m	Absorption correction	Numerical
Unit cell dimensions	a = 25.2209(5) Å b = 15.1985(3) Å c = 19.9181(4) Å β = 94.772(2) °	Max. and min. transmission	0.71272 and 1.00000
Volume	7608.5(3) $Å^3$	Refinement method	Full-matrix least-squares on F^2
Z	4	Data/restraints/parameters	7517/1075/1034
Density	1.650 g/cm^3	Goodness-of-fit on F2	0.937
Absorption coefficient	3.045	Final R indices [I > 2σ]	R1 = 0.0721, wR2 = 0.1983
F(0000)	3866	R indices (all data)	R1 = 0.0769, wR2 = 0.2034
Theta range for data collection	3.971 to 70.310 °	Largest diff. peak hole	0.657 and -1.058 e/$Å^3$
Index ranges	-23 ≤ h ≤ 30 -18 ≤ k ≤ 18 -24 ≤ l ≤ 23		

S4. UV-vis-NIR spectrum of $Sc_3N@C_{82}$ in CS_2 solution.

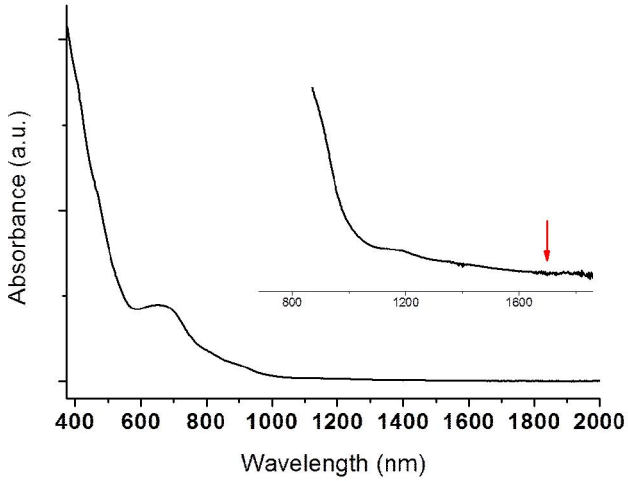

Figure S4. UV-Vis-NIR absorption spectrum of $Sc_3N@C_{82}$-C_{2v}(39718) dissolved in carbon disulfide. Inset: enlarged spectral range of 680-1860 nm and the red arrow indicated the absorption onset at 1696 nm.

Table S3. Characteristic electronic absorption data and optical bandgap ($E_{g,\ optical}$) of $Sc_3N@C_{2n}$ (2n=68, 70, 78, 80, 82) NCFs.

NCF	Absorption peaks (nm)	Absorption onset (λ_{onset}, nm)	$E_{g,\ optical}$ (eV)[a]	Ref.
$Sc_3N@C_{68}$-D_3(6140)	419, 452, 560, 600, 627, 659, 673, 729, 785, 824, 998	1200	1.10	S2
$Sc_3N@C_{70}$-C_{2v}(7854)	468, 558, 696, 807, 894	960	1.30	S1
$Sc_3N@C_{78}$-D_{3h}(5)	460, 623	1240	1.0	S3
$Sc_3N@C_{80}$-I_h(7)	424, 735	820	1.51	S4
$Sc_3N@C_{80}$-D_{5h}(6)	413, 472	950	1.30	S4
$Sc_3N@C_{82}$-C_{2v}(39718)[b]	341, 465, 642, 908	1696	0.73	This work

[a] $E_{g,\ optical}$ (eV) = 1240/λ_{onset} (nm). [b] C_{82}-C_{2v}(39718) can be also labeled as C_{82}-C_{2v}(9) according to the conventional numbering of the isolated pentagon rule (IPR) isomers based on the Fowler-Monolopoulos spiral algorithm.[S5]

S5. Thermal stability of $Sc_3N@C_{82}$ vs $Sc_3N@C_{80}$-I_h.

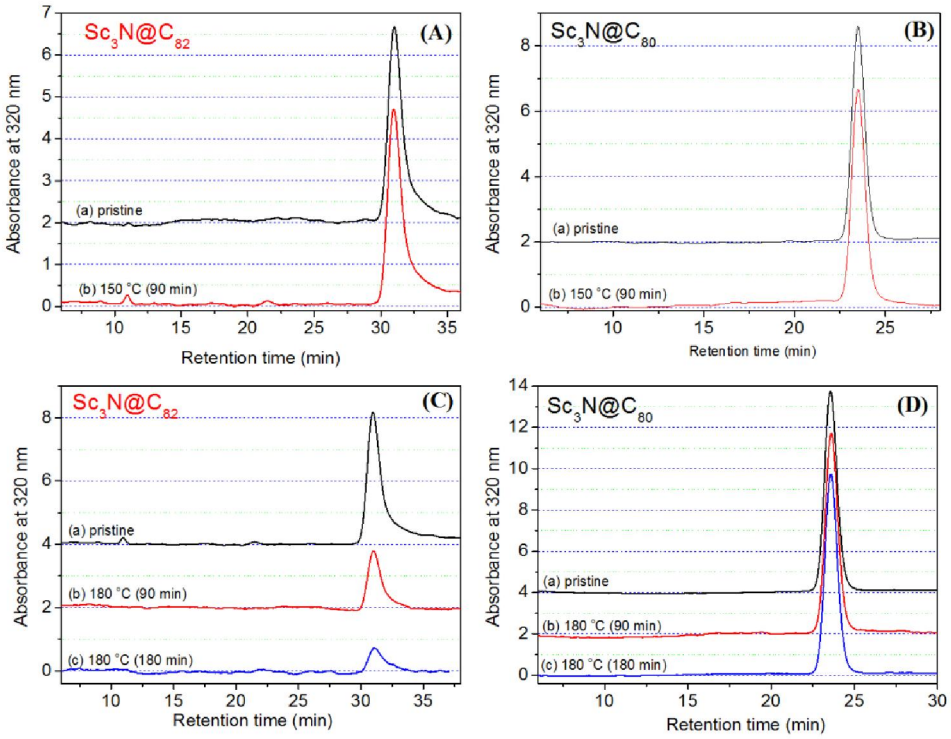

Figure S5. HPLC chromatograms of purified $Sc_3N@C_{82}$ (A, C) and $Sc_3N@C_{80}$-I_h (B, D) solutions in reflux toluene under heating at different temperature in ambient condition. (4.6 × 250 mm Buckyprep column; flow rate: 1.6 mL•min^{-1}; injection volume: 20 μL; toluene as eluent; 20 °C.)

S6. Cyclic voltammograms of $Sc_3N@C_{82}$ in different scanning regions.

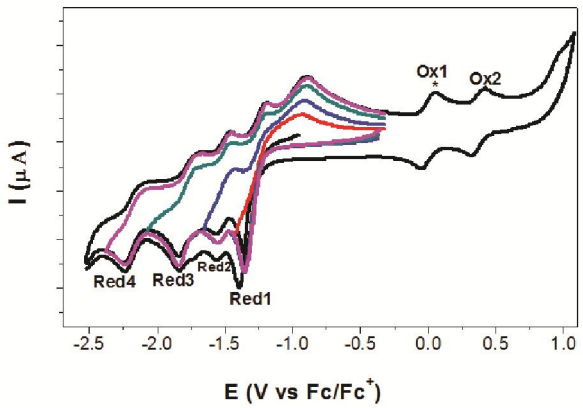

Figure S6. Cyclic voltammograms of $Sc_3N@C_{82}$-C_{2v}(39718) in *o*-DCB solution in different scanning regions showing the correlation of each reduction step with the corresponding re-oxidation step. Scan rate: 100 mV·s^{-1}, $TBAPF_6$ as supporting electrolyte. The asterisk labels the oxidation peak of ferrocene, which coincidentally overlaps with the first oxidation peak of $Sc_3N@C_{82}$-C_{2v}(39718).

Table S4. Redox potentials (V vs Fc/Fc^+) and electrochemical energy gaps ($\Delta E_{gap, EC}$) of $Sc_3N@C_{82}$-C_{2v}(39718) and $Gd_3N@C_{82}$-C_s(39663).

Samples	$E_{1/2}$ (V vs Fc/Fc^+)						$\Delta E_{gap, EC}$ / V [a]	Ref.
	Reduction steps ($E_{1/2, red}$)				Oxidation step ($E_{1/2, ox}$)			
	first	second	third	fourth	first	second		
$Sc_3N@C_{82}$-C_{2v}(39718)	-1.35[b]	-1.52	-1.78	-2.18	0	0.37	1.35	This work
$Gd_3N@C_{82}$-C_s(39663)	-1.52[b]	-1.86[b]	-	-	0.37	-	1.89	S6

[a] $\Delta E_{gap,EC} = E_{1/2,ox(1)} - E_{1/2,red(1)}$; [b] The cathodic peak potential.

References:

S1. Yang, S. F.; Popov, A. A.; Dunsch, L. *Angew. Chem. Int. Ed.* **2007,** *46,* 1256 – 1259.

S2. Yang, S. F.; Kalbac, M.; Popov, A.; Dunsch, L. *Chem. Eur. J.* **2006,** *12,* 7856 – 7862.

S3. Olmstead, M. M.; Bettencourt-Dias, A.; Duchamp, J. C.; Stevenson, S.; Marciu, D.; Dorn, H. C.; Balch, A. L. *Angew. Chem. Int. Ed.* **2001,** *40,* 1223 – 1225.

S4. Yang, S. F.; Popov, A. A.; Kalbac, M.; Dunsch, L. *Chem. Eur. J.* **2008**, *14,* 2084 – 2092.

S5. Fowler, P.; Manolopoulos, D. E. *An Atlas of Fullerenes*; Clarendon Press: Oxford, U.K., 1995.

S6. Chaur, M. N.; Athans, A. J.; Echegoyen, L. *Tetrahedron* **2008,** *64,* 11387 – 11393.